Cite this: *Chem. Commun.*, 2012, **48**, 11751–11753

www.rsc.org/chemcomm

COMMUNICATION

One-pot synthesis of responsive catalytic Au@PVP hybrid nanogels†

Chuanfu Xiao,[a] Shoumin Chen,[a] Laiying Zhang,[a] Shuiqin Zhou[b] and Weitai Wu*[a]

Received 18th August 2012, Accepted 24th September 2012
DOI: 10.1039/c2cc36002k

Responsive catalytic hybrid nanogels with Au nanoparticle cores and a polyvinylpyrrolidone (PVP) based gel shell are prepared through a novel one-pot approach. The embedded Au nanoparticles demonstrate both a pH-modulated catalytic activity and anti-aggregation properties upon recycling.

Noble metal nanoparticles and nanocomposites have received great interest due to their unique properties and applications in catalysis, photonics, electronics, and medicine.[1] One can tailor the properties of noble metal architectures and thus improve their performance by controlling their size, shape, composition, and porosity. For example, the catalytic activity of a noble metal nanoparticle is strongly dependent on its size. Typically, a smaller nanoparticle tends to show a higher catalytic activity as it has a much greater surface-to-volume ratio.[2] Having highly active surface atoms, however, often leads to changes in the size and shape of noble metal nanoparticles during catalysis and therefore a rapid decay in their catalytic abilities.[3] The challenge of preparing highly efficient catalysts based on noble metals that have an acceptable long-term stability remains to be solved.

To suppress the aggregation of noble metal nanoparticles during catalysis, two approaches are widely reported: (a) depositing them on high-surface area substances, and (b) confining them in the channels or void spaces of a porous matrix.[1,4] In both approaches, however, the slow aggregation of noble metal nanoparticles is inevitable. From a structural viewpoint, core–shell architectures with noble metal nanoparticle cores are desirable for preventing the cores from aggregation, and have therefore recently attracted a great deal of attention for catalysis application.[5] To achieve highly-efficient catalysis, the noble metal nanoparticle core should be highly accessible by reactants, whilst the shell should allow the fast diffusion of both reactants and products. Encapsulating noble metal nanoparticles in a polymer nanogel represents an effective method to create such a core–shell architecture.[6] Polymer gel is a three-dimensional cross-linked polymer network that combines the properties of solids and fluids, which gives rise to the fluid-like transport properties for the molecules significantly smaller than the gel pore size. Compared to conventional catalysts embedded in bulky supports, noble metal nanoparticle in the core–shell architectures is isolated by a highly porous gel shell and has a quasi-homogeneous surrounding environment.[7] The interaction and aggregation between noble metal nanoparticle cores can be effectively hindered. Additional advantages can be obtained if stimuli-responsive polymer gel shells are fabricated, because they offer possibilities for external switching and manipulation.[8] Such core–shell architectures for catalysis have been fabricated by multistep approaches starting from pre-synthesized noble metal nanoparticles, followed by the synthesis of a polymer gel shell using free radical polymerization, which involves the use of harsh azo initiators.[6] Although there are benefits already apparent from those approaches reported in previous arts, unfortunately, it is difficult to grow a polymer gel on the pre-designed noble metal nanoparticles of unique shapes to achieve desired catalysis performance, because the use of azo initiators can lead to passivation or even etching of the highly active surface atoms of noble metal nanoparticles.

Herein, we report a one-pot approach (Fig. 1a; see ESI† for the detailed experimental procedures) to synthesize responsive core–shell architectures comprising Au nanoparticle cores coated with a PVP-based gel shell, denoted Au@PVP hybrid nanogels. Our strategy to prepare the hybrid nanogels is based on a combination of several methods previously developed in both inorganic nanoparticle and polymer synthesis. Firstly, the use

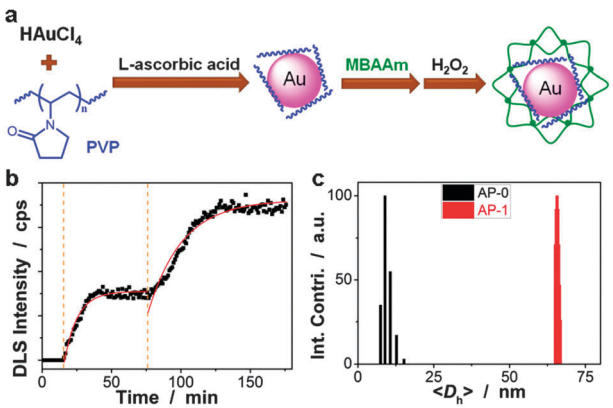

Fig. 1 (a) Schematic illustration of a one-pot approach to Au@PVP hybrid nanogels. (b) Kinetic curves of AP-1's formation. Solid lines: 1st-order kinetic fits. (c) DLS size distribution measured at pH = 6.3.

[a] *State Key Laboratory for Physical Chemistry of Solid Surfaces, The Key Laboratory for Chemical Biology of Fujian Province, and Department of Chemistry, College of Chemistry and Chemical Engineering, Xiamen University, Xiamen 361005, China. E-mail: wuwtxmu@xmu.edu.cn*
[b] *Department of Chemistry, College of Staten Island, and The Graduate Center, City University of New York, Staten Island, New York 10314, USA*

† Electronic supplementary information (ESI) available: Experimental procedures and characterization data. See DOI: 10.1039/c2cc36002k

of polymer, and in particular PVP, has proven to be extremely efficient for the synthesis of noble metal nanoparticles with a wide variety of sizes and shapes.[9] It is documented that PVP molecules can adsorb onto the growing noble metal nuclei, acting as a typical surfactant. Secondly, *interpenetrating polymer networks*, IPNs, are a broad class of polymer composites defined as a combination of two polymers in the network form.[10] Semi-IPN refers to a class of IPNs characterized by the penetration on a molecular scale of at least one of the networks by at least some of the linear or branched macromolecules. Semi-IPN can be synthesized by starting with a mixture of monomers, cross-linkers, and linear or branched macromolecules.[11] Thirdly, hydrogen peroxide, H_2O_2, an oxidizing agent, has been widely used as an initiator in free radical polymerization.[11] Recently, H_2O_2 has also been found to be a critical reagent in the synthesis of Ag nanoparticles.[12] H_2O_2 can not only improve the yield of highly anisotropic Ag nanoparticles, but also shorten the reaction time by making the aging process unnecessary, which is a great advantage in comparison to traditional seed-mediated growth methods. Typically, these different procedures can be combined in our strategy in such a way that L-ascorbic acid (6.3×10^{-4} mol), and then *N,N′*-methylenebisacrylamide (MBAAm; 1.3×10^{-4} mol) and H_2O_2 (30 wt%, 100.0 μL) were sequentially added into a mixture of $HAuCl_4$ (2.5×10^{-6} mol) and PVP (5.0×10^{-4} mol) at 25.0 °C. We monitored the whole synthesis process using *in situ* dynamic light scattering (DLS). As shown in Fig. 1b, two stages can be observed: (a) after addition of L-ascorbic acid into the mixture of $HAuCl_4$ and PVP, the DLS intensity increased immediately and then gradually flatted off; (b) the DLS intensity further increased when MBAAm and H_2O_2 were added, and became stable within 90 min. Based on the evolution of DLS intensity, apparent rate constants were derived from the fitting of the time-dependent DLS intensity with an exponential growth (k, 1st-order). The first-stage exhibited a much larger apparent rate constant k_1 of 1.18×10^{-1} min^{-1} than that of the second-stage ($k_2 = 3.85 \times 10^{-2}$ min^{-1}). Correspondingly, the average hydrodynamic diameter, $\langle D_h \rangle$, for the samples obtained at the end of the two stages was determined to be 10 nm (this sample was denoted AP-0) and 65 nm (denoted AP-1), respectively. The $\langle D_h \rangle$ distribution (Fig. 1c) shows only a single peak for narrowly distributed AP-1, as well as for AP-0, with a polydispersity index of $\mu_2/\langle \Gamma \rangle^2 \leq 0.005$. These results indicate that the gel layer has been grown onto the surface of Au nanoparticles. The coating of a gel layer also manifests as a new stretching vibration signal at 3305 cm^{-1} (N–H) and a bend vibration signal at 1535 cm^{-1} (N–H) of poly(MBAAm) in the purified AP-1 (Fig. S1 in ESI†). IR analysis also confirmed the successful interpenetrating of PVP chains into poly(MBAAm) gel networks, as revealed by the characteristic stretching vibration signals of PVP at 1287 cm^{-1} (C–N), 1665 cm^{-1} (C=O), and 2954 cm^{-1} (C–H), and a bend vibration signal at 1287 cm^{-1} (C–H) for the purified AP-1, while those signals were very weak and even undetectable for the purified AP-0. Moreover, the peak plasmon absorption of AP-1 red shifted by *ca.* 12 nm (8.5 meV) in comparison with that of AP-0 (Fig. S2 in ESI†). This red-shift in the peak plasmon absorption is related to a change in the local dielectric constant around Au nanoparticles as a result of the coating of the PVP-based gel layer onto Au nanoparticles.[13]

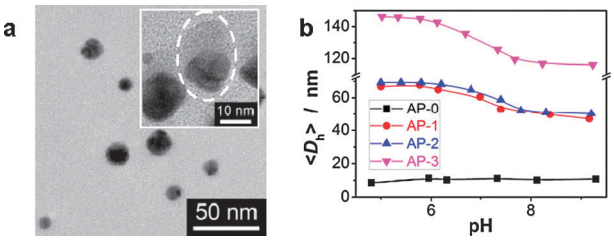

Fig. 2 (a) TEM images (AP-1) and (b) a pH-dependent $\langle D_h \rangle$ (25.0 °C) of Au@PVP hybrid nanogels.

There should be a dynamic equilibrium between the surface protection effect and the confined growth effect of the polymers on Au nanoparticles. As H_2O_2 appears to be a critical reagent for both formation of Au nanoparticles and polymerization of the gel layer,[10–12] a change in the feeding amount of H_2O_2 should be able to vary the morphology of Au@PVP hybrid nanogels. Fig. 2a shows a typical TEM image of AP-1. The markedly high electron density of Au enables direct visualization of sphere-like Au nanoparticles within a translucent gel matrix (this can be seen in the amplificatory image inset of Fig. 2a and Fig. S3 in ESI†). Interestingly, when a larger amount of H_2O_2 (30 wt%, 500.0 μL) was fed in the synthesis, the Au nanoparticle cores of the hybrid nanogels (denoted AP-2) have a polyhedron-like morphology (Fig. S3, ESI†). At a very large feeding amount of H_2O_2 (30 wt%, 5.0 mL), the Au nanoparticles within the hybrid nanogels (denoted AP-3) become dendrite-like. All the three hybrid nanogels can be well reproduced from batch to batch. While k_1 remained nearly the same, k_2 was found to exhibit the order of AP-3 (1.01×10^{-1} min^{-1}) > AP-2 (6.33×10^{-2} min^{-1}) > AP-1 (3.85×10^{-2} min^{-1}) (see Fig. S4 and S5 in ESI† for kinetic curves of the synthesis of AP-2 and AP-3, respectively). All hybrid nanogels show good stability. No sediment was observed after 2 months' storage at *ca.* 25.0 °C.

To be an efficient catalyst, the shell of core–shell architectures should be so permeable to both reactants and products that mass-transfer limitations can be avoided to maximize the reaction rates. The high porosity of the gel layer in the Au@PVP hybrid nanogels is then crucial for their catalysis applications. The pH-responsive swelling–deswelling transition behaviour (Fig. 2b) does confirm the highly porous nature of the gel layer. At pH > 8.0, the size of the hybrid nanogels remains nearly a constant; when pH ≤ 8.0, the size gradually increases until pH < 6.0, where the hybrid nanogels reach a maximum swelling. This swelling–deswelling transition pH region is close to the hydrophilic–hydrophobic transition pH region (centred at 7.5) of the PVP film determined by using contact angle measurements.[14] It is reported that at a high pH value above the transition region, the PVP film is relatively hydrophobic; as the pH value decreases, it becomes more hydrophilic. The swelling ratio, $\langle D_h \rangle_{pH=5.0}/\langle D_h \rangle_{pH=9.3}$, was found to exhibit the order of AP-1 (1.42) > AP-2 (1.38) > AP-3 (1.26). In contrast, the $\langle D_h \rangle$ of AP-0 remained nearly constant of *ca.* 10 nm, indicating good stability of Au nanoparticles in our experimental pH window (5.0–9.3). Therefore, these results can not only provide direct proof on the high porosity of the hybrid nanogels, but also foreshadow a novel responsive system for pH-modulated catalysis.

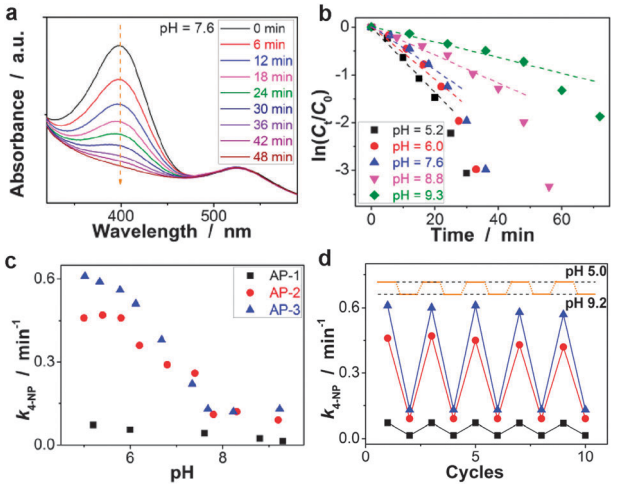

Fig. 3 (a) Time-domain UV-vis spectra of the reaction mixture during the course of reduction of 4-NP, and (b) influence of pH value on $k_{4\text{-NP}}$, measured with AP-1. (c) The $k_{4\text{-NP}}$–pH plot showing the pH-modulated catalytic activity. (d) A comparison of catalytic activity during five cycles of use: ■, AP-1; ●, AP-2; and ▲, AP-3.

We performed the catalytic reduction of 4-nitrophenol (4-NP) by $NaBH_4$ (Fig. 3a),[1e] which does not progress at 25.0 °C without the use of catalyst in the pH range of 5.0–9.3 (Fig. S6 in ESI†), in order to evaluate the accessibility and catalytic performance of Au nanoparticles in Au@PVP hybrid nanogels. Since the concentration of $NaBH_4$ (4.7×10^{-3} M) exceeds that of 4-NP (C_t at the reaction time t, and $C_0 = 3.2 \times 10^{-5}$ M at $t = 0$), the reaction should be of pseudo first order with regard to this reactant. Fig. 3b shows that this is the case for solution pH ranging from 5.0 to 9.3 (see Fig. S7 and S8 in ESI† for the cases using AP-2 and AP-3, respectively). Linear relationships between $\ln(C_t/C_0)$ and t are obtained in all cases at low conversions. Deviations from linearity are only seen for high degrees of conversion (>75%). This finding is in accord with the catalysis of this reaction by Ag nanoparticles in Ag@polymer hybrid nanogels.[5a] However, for the present purpose it suffices to discuss the initial rates of reaction. The reaction rate constant $k_{4\text{-NP}}$ for the reduction of 4-NP by AP-1, AP-2, and AP-3 (3.0×10^{16} Au-atoms per mL; at pH 5.0) is calculated to be 7.2×10^{-2} min, 4.6×10^{-1} min, and 6.1×10^{-1} min^{-1}, respectively, indicating a highly efficient catalytic activity. This increase in catalytic activity should be due to an increase in the specific surface area of Au nanoparticle cores.

The $k_{4\text{-NP}}$ obtained from these plots are shown in Fig. 3c, and it is interesting to note that the $k_{4\text{-NP}}$ obtained at different pH values mirror the typical dependence of $\langle D_h \rangle$ on the pH value (Fig. 2b). When the pH value is low, the hybrid nanogels are totally swollen with water. In this case the Au nanoparticles which have been embedded within the gel layer are fully accessible to the reactants for the catalytic reduction. However, when the pH value is higher than *ca.* 6.0, the hybrid nanogels shrink markedly with an increase in pH. The shrinking of the gel layer resulting from the expulsion of water is followed by a concomitant slowing down of the diffusion of reactants within the gel. This process will in turn lower the rate of the reaction catalyzed by Au nanoparticles. The reaction rate lowers down to nearly a minimum if the pH value is increased further to above *ca.* 8.0, where the $\langle D_h \rangle$ of the hybrid nanogels stays constant. It seems as if the $k_{4\text{-NP}}$ exhibited an opposite dependence of the thickness of the gel layer on the pH value. Actually, the change in the $k_{4\text{-NP}}$ by the diffusion path length may have been overcompensated by the permeability of the gels.[5a,6,7] Moreover, the hybrid nanogels were separated by centrifugation, purified by dialysis, and then redispersed into fresh solution. The cycled hybrid nanogels exhibit similar catalytic activity to the initial ones (return to >90% of original $k_{4\text{-NP}}$ values; Fig. 3d), due to the anti-aggregation properties of Au nanoparticle cores and the reversible swelling–deswelling transition of the gel layer.

In conclusion, we have developed a one-pot synthetic approach to prepare responsive catalytic Au@PVP hybrid nanogels. With significant advances achieved in polymer-assisted synthesis of noble metal nanoparticles, we anticipate that this new approach may serve as a good starting point for the synthesis of stable, efficient, and reversible hybrid nanogel catalysts with a huge potential in a wide range of fields.

This work is supported by the NSFC (21274118), the FRFCU (2012121016), the NFFTBS (J1030415), and the NCETFJ.

Notes and references

1 (*a*) J. Zeng, Q. Zhang, J. Y. Chen and Y. N. Xia, *Nano Lett.*, 2010, **10**, 30; (*b*) N. J. Halas, *Nano Lett.*, 2010, **10**, 3816; (*c*) B. Wanjala, B. Fang, J. Luo, Y. Chen, J. Yin, M. Engelhard, R. Loukrakpam and C. J. Zhong, *J. Am. Chem. Soc.*, 2011, **133**, 12714; (*d*) K. D. Osberg, M. Rycenga, N. Harris, A. L. Schmucker, M. R. Langille, G. C. Schatz and C. A. Mirkin, *Nano Lett.*, 2012, **12**, 3828; (*e*) P. Hervés, M. Pérez-Lorenzo, L. M. Liz-Marzán, J. Dzubiella, Y. Lu and M. Ballauff, *Chem. Soc. Rev.*, 2012, **41**, 5577.

2 X. Q. Huang, C. Y. Guo, J. Q. Zou, N. F. Zheng and G. D. Stucky, *Small*, 2009, **5**, 361.

3 A. Roucoux, J. Schulz and H. Patin, *Chem. Rev.*, 2002, **102**, 3757.

4 (*a*) D. Astruc, F. Lu and J. R. Aranzaes, *Angew. Chem., Int. Ed.*, 2005, **44**, 7852; (*b*) G. A. Somorjai and R. M. Rioux, *Catal. Today*, 2005, **100**, 201.

5 (*a*) Y. Lu, Y. Mei, M. Drechsler and M. Ballauff, *Angew. Chem., Int. Ed.*, 2006, **45**, 813; (*b*) Y. D. Yin, R. M. Rioux, C. K. Erdonmez, S. Hughes, G. A. Somorjai and A. P. Alivisatos, *Science*, 2004, **304**, 711; (*c*) M. Casavola, R. Buonsanti, G. Caputo and P. D. Cozzoli, *Eur. J. Inorg. Chem.*, 2008, 837; (*d*) J. Bao, J. He, Y. Zhang, Y. Yoneyama and N. Tsubaki, *Angew. Chem., Int. Ed.*, 2008, **47**, 353; (*e*) S. Takenaka, H. Umebayashi, E. Tanabe, H. Matsune and M. Kishida, *J. Catal.*, 2007, **245**, 392; (*f*) J. Lee, J. C. Park and H. Song, *Adv. Mater.*, 2008, **20**, 1523; (*g*) J. P. Ge, T. Huynh, Y. X. Hu and Y. D. Yin, *Nano Lett.*, 2008, **8**, 931.

6 S. Carregal-Romero, N. J. Buurma, J. Pérez-Juste, L. M. Liz-Marzán and P. Hervés, *Chem. Mater.*, 2010, **22**, 3051.

7 Y. Lu, S. Proch, M. Schrinner, M. Drechsler, R. Kempe and M. Ballauff, *J. Mater. Chem.*, 2009, **19**, 3955.

8 C. Wu and S. Q. Zhou, *Phys. Rev. Lett.*, 1996, **77**, 3053.

9 Y. N. Xia, Y. J. Xiong, B. Lim and S. E. Skrabalak, *Angew. Chem., Int. Ed.*, 2009, **48**, 60.

10 T. Tominaga, V. R. Tirumala, S. Lee, E. K. Lin, J. P. Gong, H. Furukawa, Y. Osada and W. Wu, *J. Phys. Chem. B*, 2008, **112**, 3903.

11 W. T. Wu, M. Aiello, T. Zhou, A. Berliner, P. Banerjee and S. Q. Zhou, *Biomaterials*, 2010, **31**, 3023.

12 Q. Zhang, N. Li, J. Goebl, Z. D. Lu and Y. D. Yin, *J. Am. Chem. Soc.*, 2011, **133**, 18931.

13 P. Mulvaney, *Langmuir*, 1996, **12**, 788.

14 S. Demiric, A. Alaslan and T. Caykara, *Appl. Surf. Sci.*, 2009, **255**, 5979.